JKAU: Eng. Sci., vol. 5, pp. 77-94 (1413 A.H. / 1993 A.D.)

Factors Affecting Optical Detection of Corona Discharges in SF_6

A.H. MUFTI,
Elect. Dept & Comp. Eng., Faculty of Engineering, King Abdulaziz University, Jeddah, Saudi Arabia

D.F. BINNS
Elect. Dept & Electronics Eng., Faculty of Engineering, University of Salford, Salford, U.K.

and

N.H. MALIK
Elect. Eng. Dept, College of Engineering, King Saud University, Riyadh Saudi Arabia

ABSTRACT. This paper describes an optoelectronic system for detecting corona discharge in SF_6 filled systems. Using the discharge detection system, investigations have been carried out to study the influence of various experimental parameters on the amount of detected corona light. It is shown that the measured irradiance due to corona depends upon the applied voltage level, gas pressure, the distance and angle between the corona source and the fibre optic light guide, and the radius, the material as well as surface properties of the electrodes. It is further shown that addition of nitrogen to SF_6 significantly improves the corona light emission. The sensitivity of the detection system can be further improved by the use of fluorescent paint on the interior walls of the pressure vessel.

1. Introduction

SF_6 gas has excellent electrical, chemical and thermal properties and is extensively being used as an insulating and arc quenching medium in compressed gas insulated systems (GIS). The major drawback of this gas is its high sensitivity to the presence of microscopic regions of high field. Such regions may occur due to the presence of foreign free and fixed metallic and non-metallic particles as well as electrode and insulator surface imperfections. The surface roughness in an industrially finished conductor system typically results in a reduction of the insulation strength of SF_6 to about half of the theoretical strength, whereas a contaminating particle can cause breakdown at fields considerably lower than this, reducing the insulation level by as much

as 90%[1,2]. As a result of such conditions, several types of discharges can occur in GIS. If such discharges go undetected, these can lead to ultimate failure of the insulation. Therefore, in order to improve the life and system reliability, there is considerable interest in the early detection and consequent prevention of partial discharges of SF_6 insulated systems.

The discharge detection methods can be broadly classified as chemical[3-6], acoustic[7-10], electromagnetic[3,11-12], electrical[7,13-14] and optical[3,15-16].

The optical method being based on the detection of emitted radiation during the discharge, it is potentially very attractive for GIS as it is not affected by any external electrical and mechanical noise as in the electrical and acoustic methods, respectively. Where as considerable qualitative information have been reported in the literature[17-19] about the temporal and spatial characteristics of corona in SF_6 gas and its mixtures with other gases, there is still a strong need for a better understanding of the emission behavior of different discharge modes in SF_6 gas and the influence of various experimental parameters on such characteristics.

This paper describes an optoelectronic discharge detection system. Using the system, positive corona discharges have been investigated in SF_6 gas and its mixtures with several other gases under different experimental conditions in order to obtain a better understanding of the factors which can influence the sensitivity of optical discharge detection. The paper reports on the results of such investigations.

2. Experimental System and Procedures

Positive AC corona was studied using the electrode arrangements shown in Fig. 1. The steel pressure vessel was 20 cm in diameter and 20 cm in height. A point electrode was mounted to the incoming high voltage connection with the axis of the point directed towards the optical guide (Fig. 1(a)) or at right angle to it (Fig. 1(b)). Tests were also carried out using a 17 cm long 25/75 mm diameter concentric cylindrical arrangement incorporated within the pressure vessel as shown in Fig. 1(d). Figure 1(c) shows an arrangement where an insulator barrier is located between the point electrode and the optical guide. A regulated HVAC power source was used. Highly polished conical point electrode each being 5 cm long and 1 μm tip diameter made from aluminium or brass were used as the corona point. The high voltage conductors used in the coaxial arrangement were also made from brass or aluminium and had different surface finishes.

An optical window was included in the pressure vessel. From the window, the light entered a fibre optic (F.O.) light guide through a Fafnir bearing. The Fafnir bearing is a fabric lined, metal backed, bearing which is light proof and gas tight, and, provides a simple, flexible and economical means to view a large area inside the vessel from a given window by simply adjusting the cone angle to the optic waveguide. The bearing used allowed the axis of the optical guide to rotate in a conical volume of 30 degrees half angle. From the fibre optic light is detected by a photomultiplier (PM) tube. The PM tube was used with a control unit containing an amplifier and a digital

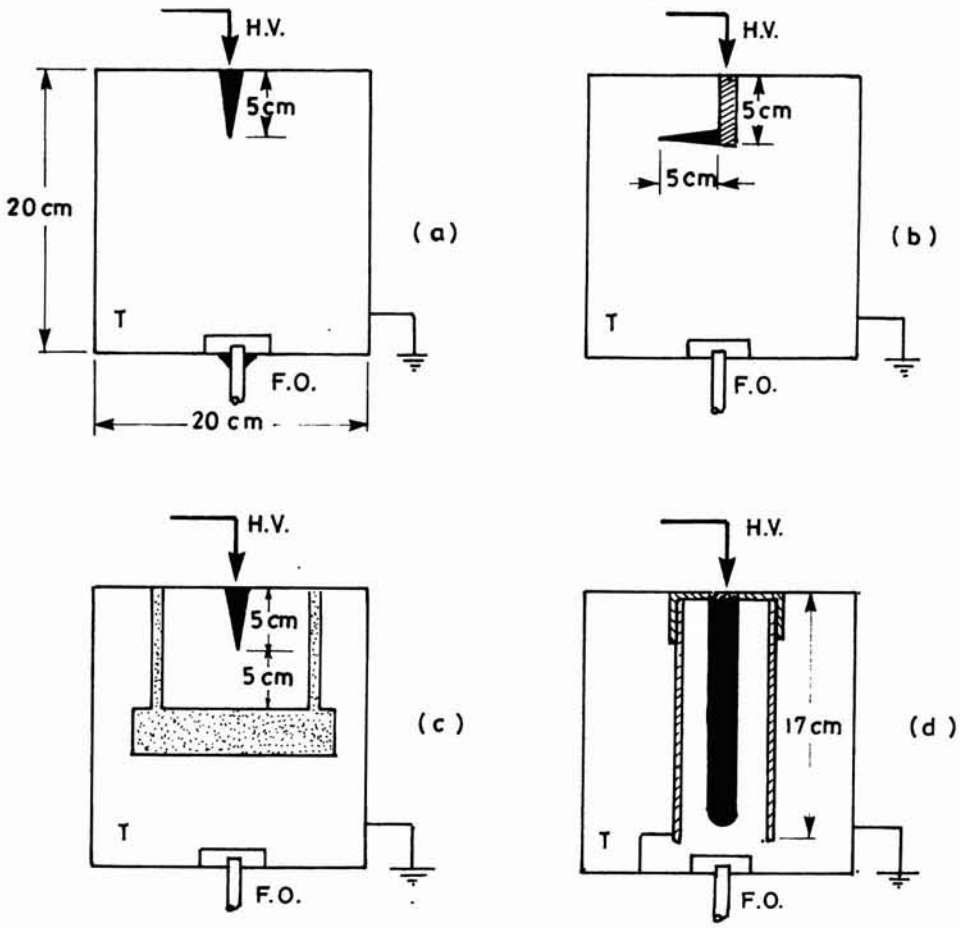

FIG. 1. Different electrode arrangements.

display unit. The Binary-coded-decimal (BCD) output of the display unit gave light quantity averaged over 0.45 s. A series of such outputs was fed to a BBC (Acorn) computer programmed to analyse 40 reading taken over a period of 18 s for a constant applied voltage. Each measurement was repeated in this fashion three times in 1 kV voltage steps. The results given here are the average of all 120 measurements for a given set of experimental conditions. The light output was measured as irradiance in five decades ranges (2×10^{-14} W/cm^2 to 2×10^{-10} W/cm^2).

The optical window was made of quartz (fused silica), and was 50 mm in diameter and 6 mm thick. Its spectral response was in the range of 120 nm and 4500 nm (10% cut off points). A 2 m long 3.5 mm diameter glass fibre light guide with a spectral range of 400 to 2400 nm was used. The PM tube used was Hamamatsu side-on with multialkali cathode material having a photocathode area of 24×8 mm^2. The spectral response of the photocathode was approximately from 200 nm to 800 nm with 330 nm

as the peak response wavelength. The current amplification the the PM tube was 5×10^6. The PM tube was operated at ambient temperature. The system was calibrated at 300 nm.

3. Results and Discussion

3.1 Effect of Electrode Position

The amount of discharge light received by the optical detector greatly depends upon the position of the discharge source with respect to the optical guide. In Fig. 1(a), the corona point is directed straight along the optical window, whie in Fig. 1(b), it is at right angle to the window. Thus these two electrode positions give different light emission angles according to received cone angle of the fibre optic. In position (a), the light beam is directed at the fibre optic cone angle with a very small background reflection. In position (b), the corona light is not directed at the cone angle and the light received depends to a large extent on partial background reflection. In both positions, the radiant power proceeds from a point source of light and obeys the inverse square law and the cosine law for irradiance measurements. In position (c), an insulating barrier is located between the corona source and the fibre optic light guide to only allow reflected light from the discharge to the measured. Figure 2 shows the light irradiance measured as a function of applied voltage for different positions of corona point with respect to the light guide. This figure clearly shows that the maximum irradiance is measured when the light guide is directed towards the discharge source (curve (a)). As the light guide is rotated away from the discharge source the irradiance level decreases as shown in curve (b). Minimum irradiance is measured when the discharge source is hidden behind the barrier (curve (c)). In this case the measurement of irradiance is due to reflected light only. For positions (a), (b) and (c), the corona light was detected at threshold voltages of 18, 20 and 35 kV, respectively. Therefore, the differences observed in the threshold voltage levels are due to insufficient light available at the light guide input.

For the electrode arrangement of Fig. 1(a), the total light measured while pointing the fibre optic light guide in different directions is shown in Fig. 3. It is clear that as the fibre optic is directed away from the discharge source, the irradiance magnitude is reduced. This property can be used in locating the discharge source.

It is important to note that, in case of curve (c), the measured irradiance is due to reflected light only. It should be pointed out that the corona point used had a tip diameter of 1 μm. For such a sharp point, the field decreases very rapidly with distance away from the tip. Consequently, the active discharge volume is very small and the discharge magnitude in terms of charge as well as light emission is very small. It should be further pointed out that for such a sharp point, the corona inception voltage does not vary with gap length in any significant manner. Thus, the discharge inception voltages for the three point positions are expected to be roughly similar[19,20].

3.2 Effect of Applied Voltage

The corona light increases with applied voltage above the threshold level as shown

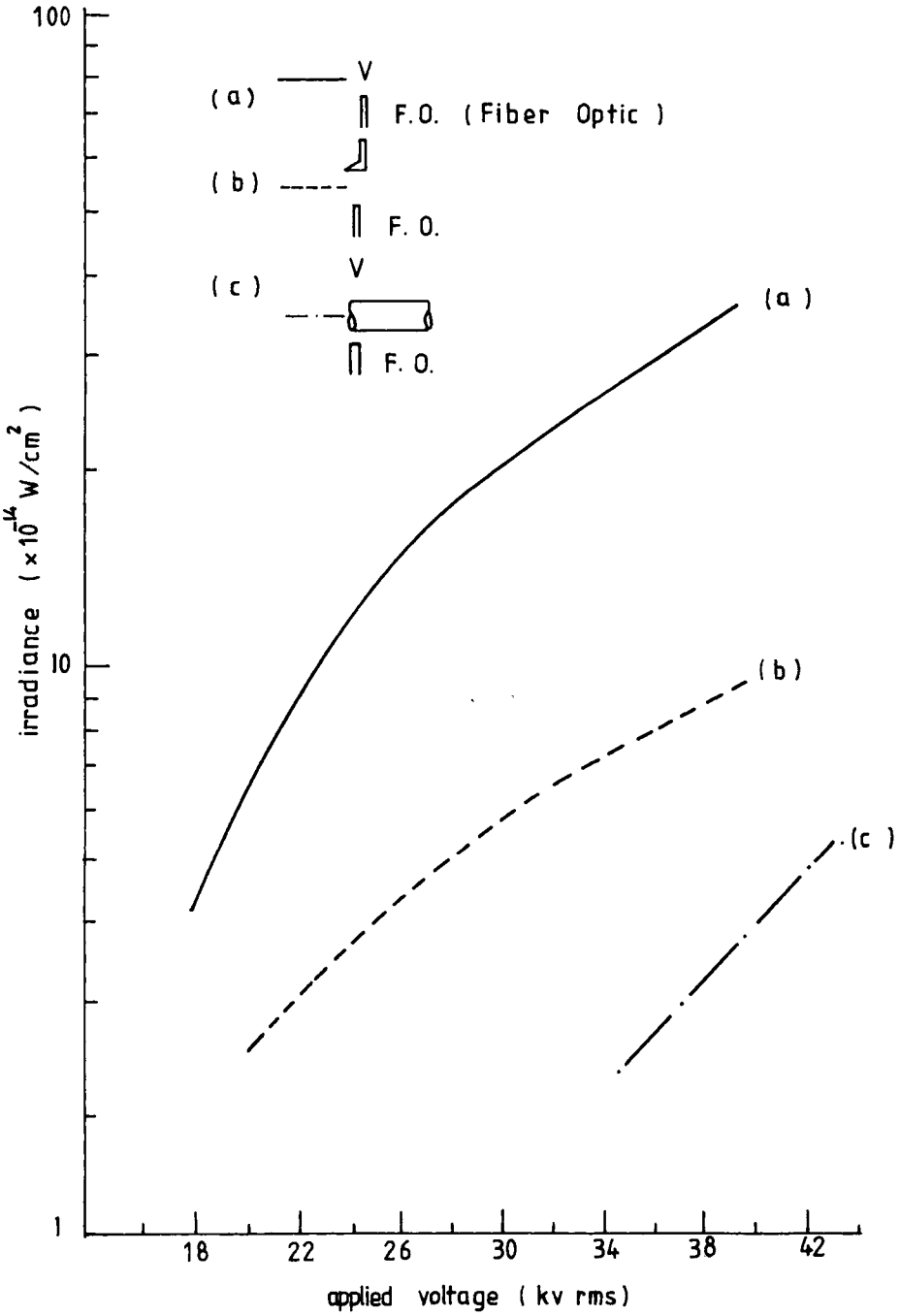

FIG. 2. Corona light emission in SF_6 at 3 bars.

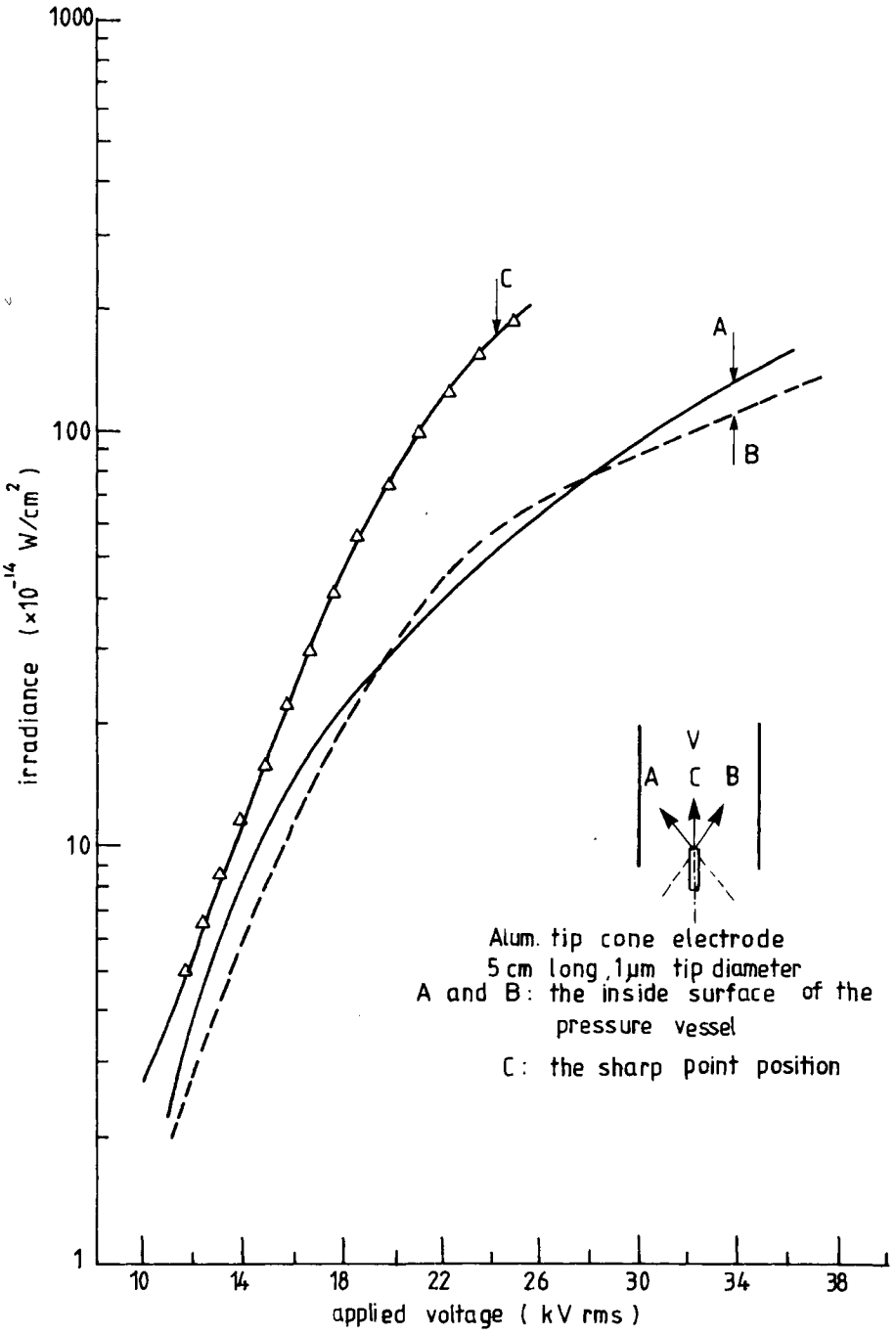

FIG .3. Variation of light intensity with applied voltage and the angle of light guide.

earlier in Fig. 2 and 3. Based upon numerous such measurements it was observed that generally the variation of the light intensity with applied voltage can be expressed according to a mathematical relation. Taking the intensity I_0 at voltage V_0 as a threshold, the intensity I at a voltage V can be approximated as follows

$$I = I_0 \cdot 10^{(V - V_0)V_0} \tag{1}$$

In these tests I was generally in the range of 1 to 10×10^{-14} W/cm^2, and I ranged from 1 to 1000×10^{-14} W/cm^2. This equation implies a tenfold increase in the light intensity when the voltage is doubled in reference to the threshold level.

It is important to point out that the light irradiance for corona in SF_6 is usually very small. This is due to the fact that in SF_6 at 3 bars, stable glow corona such as that observed in air does not occur. At its inception, the corona is in the form of intermittent burst pulses. As the voltage is further increased, the pulse level as well as pulse repetition rate increase giving it the appearance of a continuous discharge. Thus, the total corona light increases with the applied voltage.

3.3 Effect of Gas Pressure

The gas pressure has significant influence on both the nature of the corona phenomena as well as the level of the light emission associated with such a discharge. Figure 4 shows the light irradiance in SF_6 at gas pressures of 3 and 2 bars for the electrode arrangement of Fig. 1(b). It is clear from this figure that the radiant intensity decreases by an increase in the gas pressure. This is due to the following main reasons ;

a) As a result of increasing gas pressure, large and infrequent discharges occur instead of a continuous discharge. Furthermore, the duration of burst pulses decreases and such pulses become quite narrow for a pressure above 4 bars. Thus, the average irradiance of emitted light decreases with pressure.

b) When light travels in the gaseous media, it is partially absorbed by the medium. The photon beam intensity I in the gas at a distance x from the source is given by

$$I = I_0 e^{-kx} \tag{2}$$

where I_0 is the beam intensity at $x = 0$ and k is the photoabsorption coefficient of the gas. k depends upon the light wavelength, gas type as well as gas pressure. It increases with gas pressure, thereby, reducing the photon's mean free path at high pressures.

Thus, the received light by the PM detector will decrease with an increase in the gas pressure as well as distance between the corona source and the receiving light guide.

3.4 Effect of Fluorescent Paint

SF_6 emits considerable portion of the radiation in the U.V. (ultra violet) and near U.V. range[19]. It appears that the relative portion of the emission in the visible range

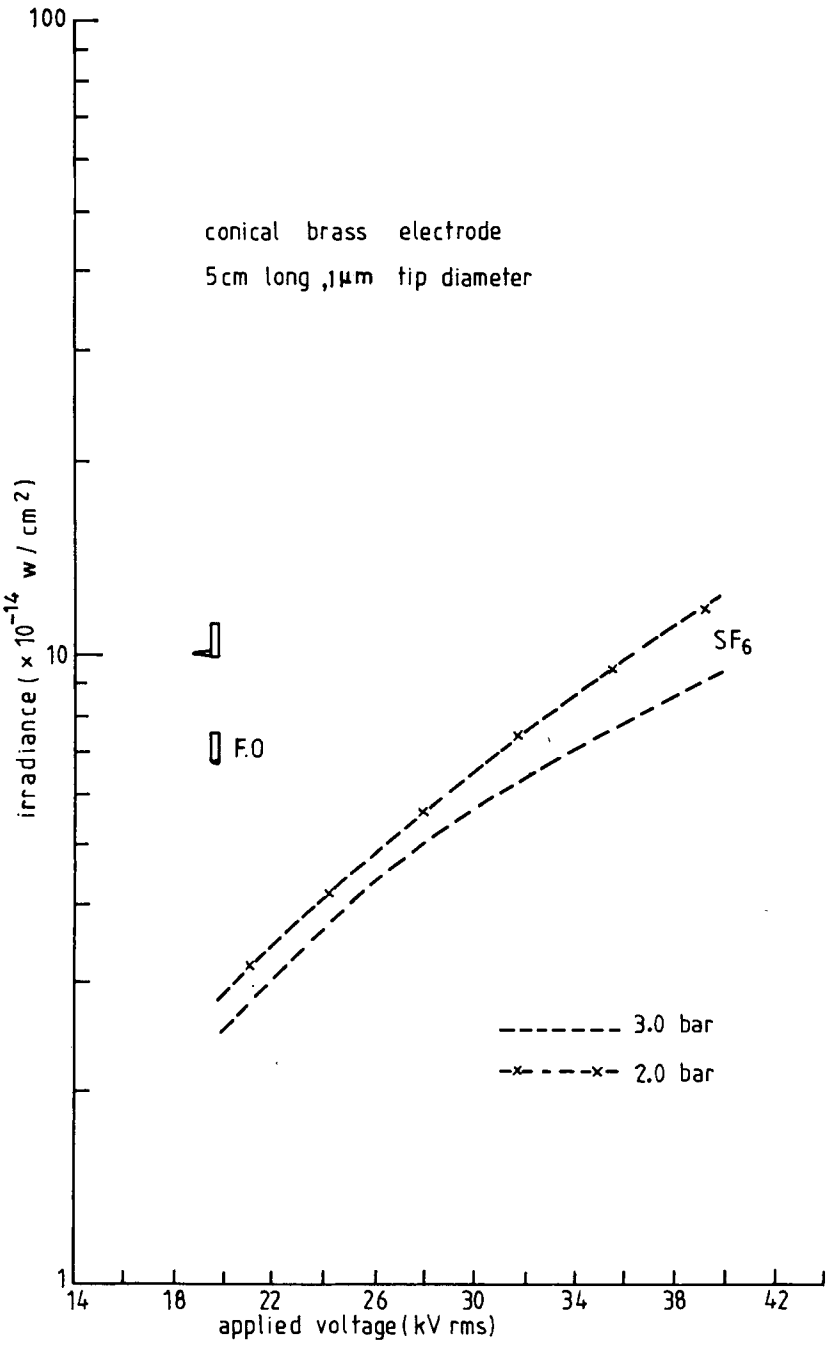

FIG. 4. Effect of gas pressure on corona light detected in SF_6.

to that in the U.V. range increases with the applied voltage. Therefore, to detect the discharge near its inception, it is preferable to have a system which can detect U.V. light with better sensitivity. This may be achieved by using suitable fluorescent paint on the walls of the pressure vessel to absorb the ultraviolet light from the corona discharge and re-emit it as visible light. Such a paint can also improve the light reflection from the vessel walls. Figure 5 shows the effect of a blue/blue fluorescent paint on the corona light emission characteristics for electrode arrangement of Fig. 1(a). It is clear from this figure that use of such a paint helps considerably to detect the discharge at an early stage. Similar results were observed for other electrode arrangements.

3.5 Effect of Electrode Material

The material of the active electrode may influence the corona light since light emission under the corona discharge is considered quite likely to contain to some degree the spectra of the electrode material used. The basic material used in GIS is an aluminium alloy. Figure 6 shows the characteristics of detected corona light for two similar points made from brass and aluminium in SF_6 and SF_6-N_2 mixtures. With aluminium point, the irradiance is 2-3 times higher and the threshold voltage is lower. This figure suggests that part of corona light is indeed due to spectra of active electrode material. It has also been observed that the light spectrum for corona in air with aluminium electrode has more spectral lines over a wider wavelength range as compared to the spectrum measured for brass electrode under otherwise similar experimental conditions[20]. In the present experiments it was further observed that sharp points made from alimunium had generally higher irradiance levels as compared to similar sharp points made from brass. This was also true for coaxial electrode system for both SF_6 and SF_6-N_2 mixtures. Since GIS are usually constructed from aluminium, it is anticipated that the active discharge point will also be of the same material. This could result in an increased detection sensitivity for the optical detectors when applied to practical GIS.

3.6 Effect of Electrode Surface

In order to investigate the influence of electrode surface finish, the coaxial system of Fig. 1(d) was used. A standard aluminium rod with a usual industrial finish without any deliberately created sharp points on its surface was used. The ground cylinder used was also smooth. With SF_6 at 3 bars, as the voltage was increased, light was observed at a threshold voltage of 45 kV with an irradiance magnitude of 2.5×10^{-14} W/cm^2. As the fibre optic was swivelled to view both sides of the HV conductor, it was observed that on side (A) had irradiance of 1.7×10^{-14} W/cm^2 whereas the other side (B) had irradiance of 4.8×10^{-14} W/cm^2. This indicated that the discharge sources on side (B) were either more in number or severity. This is due to the presence of some sharp points on one side of the high voltage rod.

When the high voltage rod was changed to a smooth rod, no light could be observed in SF_6. When 63% SF_6 + 37% N_2 mixtures were used instead of pure SF_6, more light was observed for a standard aluminium rod as compared to the smooth

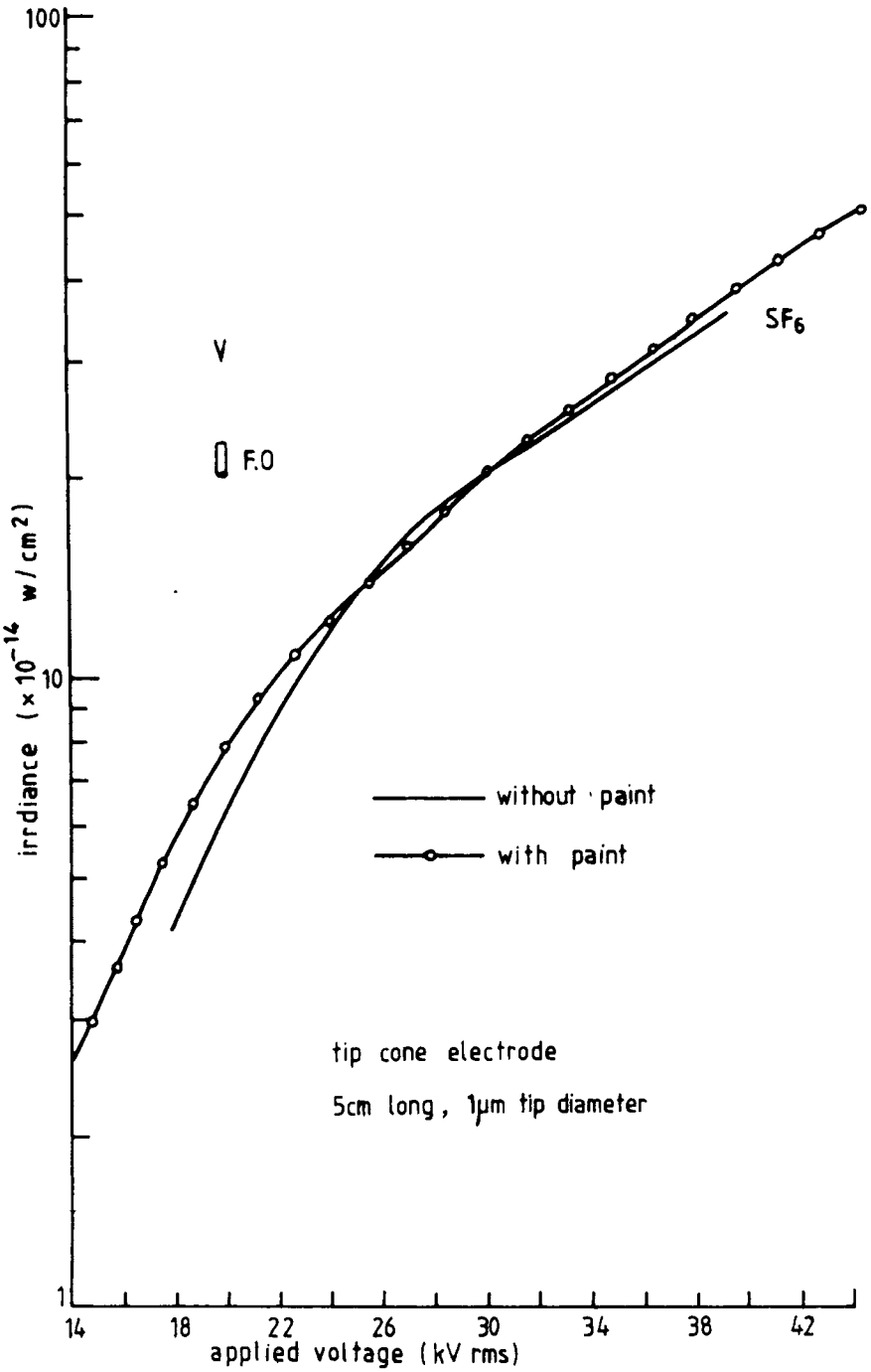

FIG. 5. Effect of fluorescent paint (blue/blue) on the corona light characteristics at 3 bars.

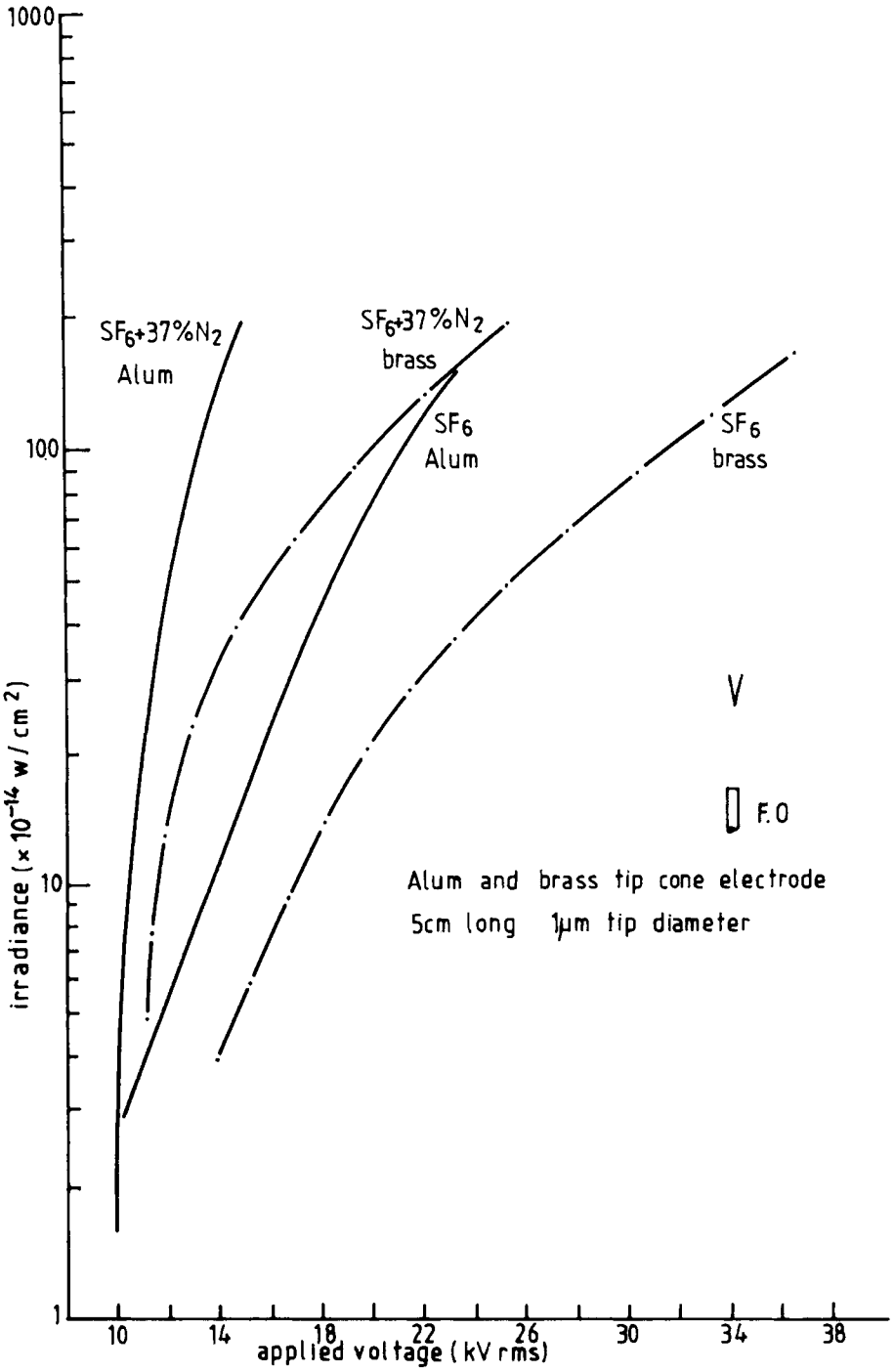

FIG. 6. The effect of electrode material on the corona light at 3 bars.

rod. Thus, the effect of surface roughness is apparent.

The effect of electrode surface finish was further investigated by deliberately introducing protrusions on the inner surface of the grounded cylinder as well as on the outer surface of the high voltage conductor. With such an arrangement, the light emission was detected at an early stage. The total light depended upon several factors such as applied voltage, gas pressure, size of the protrusion, location of the protrusion (high voltage bus or the ground conductor), material of the protrusion (brass or aluminium), material and surface finish of the coaxial electrodes as well as the angle and the distance between the discharge source and the light guide. Figure 7 shows some typical results using an aluminium protrusion on the grounded aluminium cylinder and smoothed brass or aluminium rods as the high voltage electrode. It may be noted that the surface finish of the electrodes influences the discharge light in two ways. Firstly, the surface roughness results into microscopic regions of high field which may become sources of discharge and, therefore, will tend to increase the detected light. Secondly, a rough surface has a smaller coefficient of reflection for light that may fall on such a surface. This is due to the random scattering from rough surface. Therefore, it tends to decrease the total detected light. Hence, the overall influence of surface finish will be due to the net result of both of these factors.

3.7 Effect of Gas Additives

In order to simulate corona discharges that may occur in a hidden area in a GIS, irradiance measurements were carried out using the electrode arrangement of Fig. 1(c) where an insulating barrier is located between the electrode and the optical window to allow only reflected light to be measured. In SF_6 at 3 bars, when the voltage was raised to 35 kV, the discharge threshold was observed with irradiance of 2.5×10^{-14} W/cm^2. However, there was significant variation in the irradiance magnitude.

In order to increase the effectiveness of the optical detection as well as optical detection range, it may be possible to increase the corona light emission in SF_6 by using small amounts of suitable gas additives. Such gas mixtures should have electrical, chemical and thermal characteristics similar to SF_6 but should improve the light emission. Nitrogren appears to be one such additive since SF_6/N_2 mixtures with high SF_6 content have dielectric strength which is approximately similar to that of SF_6. Therefore, mixtures of SF_6 with nitrogen were investigated from the optical discharge detection point of view. In addition, mixtures of SF_6 with gases such as He, Ar and Ne which are commonly used in discharge lamps were tested. Figure 8 shows the measured irradiance levels for SF_6 and its mixtures with other gases. This figure also shows the corona light measured for the additive gases alone at a pressure of 0.3 bar. It is interesting to note that, when tested alone, Ne has the highest corona light irradiance and exhibits the lowest threshold voltage level. On the other hand, N_2 has the highest threshold voltage level and the lowest irradiance magnitude. However, among mixtures of SF_6 with these gases, SF_6-N_2 mixtures exhibit the lowest threshold voltage and significantly higher irradiance levels. Thus, the addition of nitrogen to

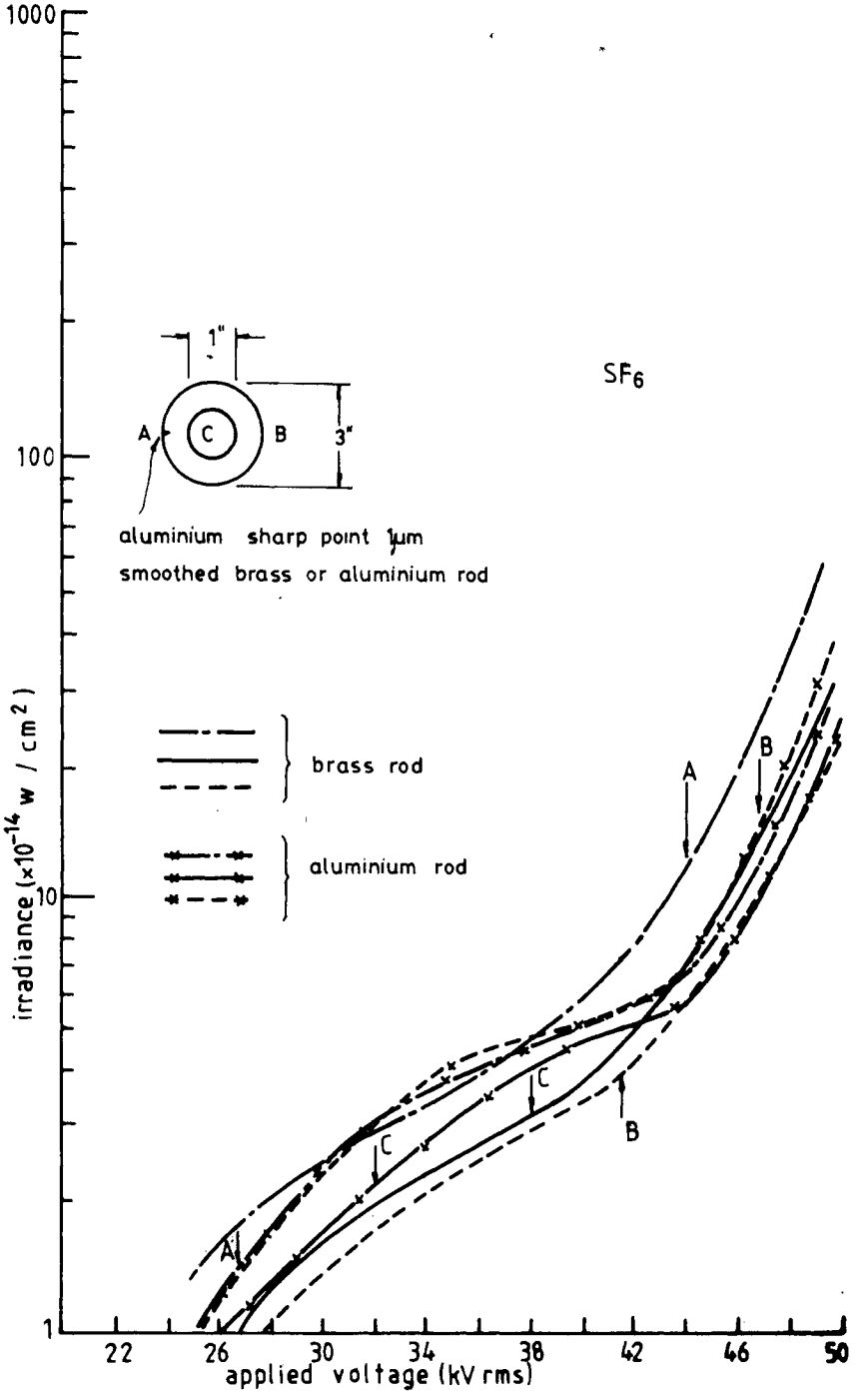

FIG. 7. Characteristics of the detected light for an aluminium protrusion and brass and aluminium rods in a 25/75 mm coaxial system with SF_6 at 0.3 bars.

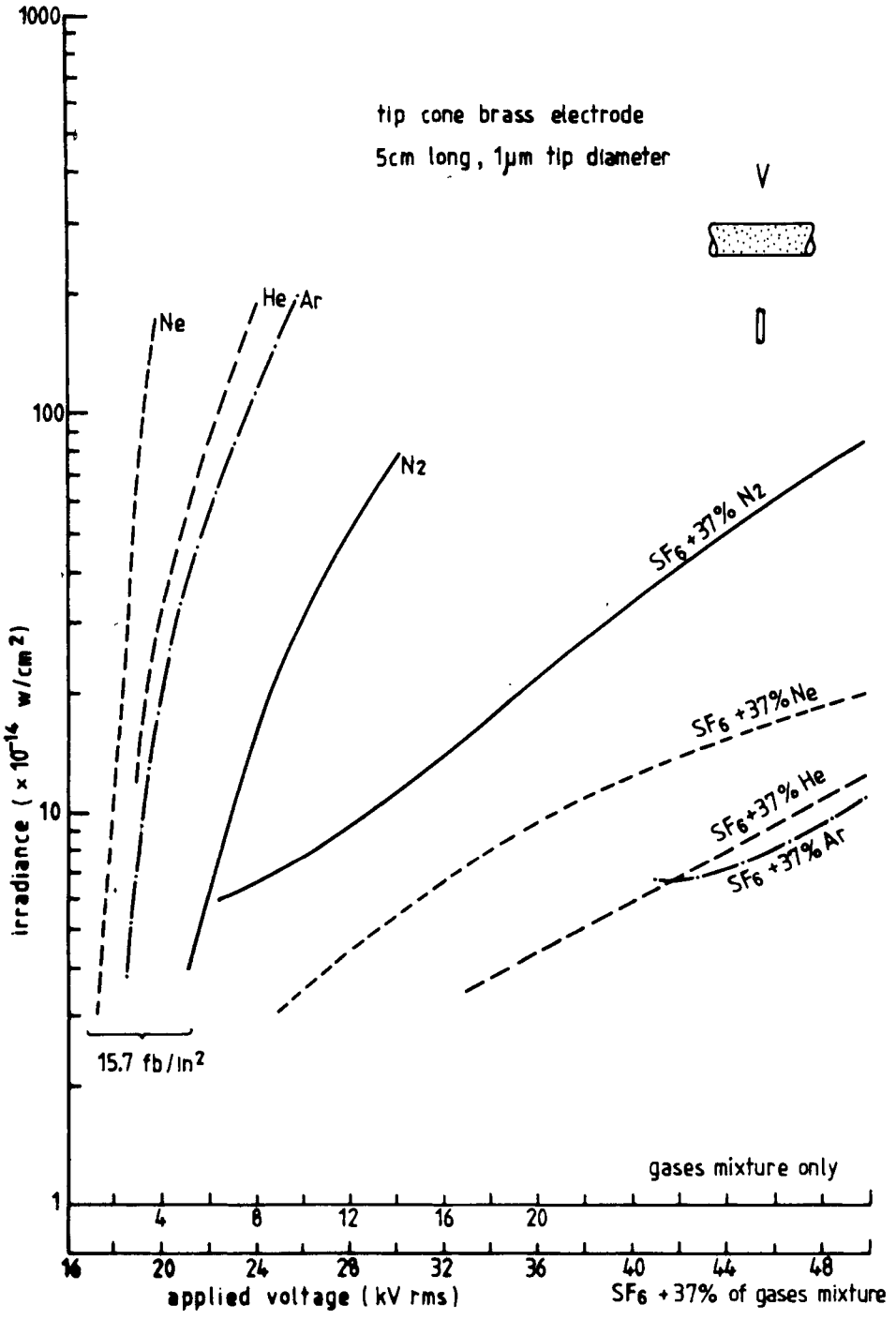

FIG. 8. Corona light characterstics for some gas additives (at 1 bar pressure) and SF_6 mixtures with these additives of 0.3 bars.

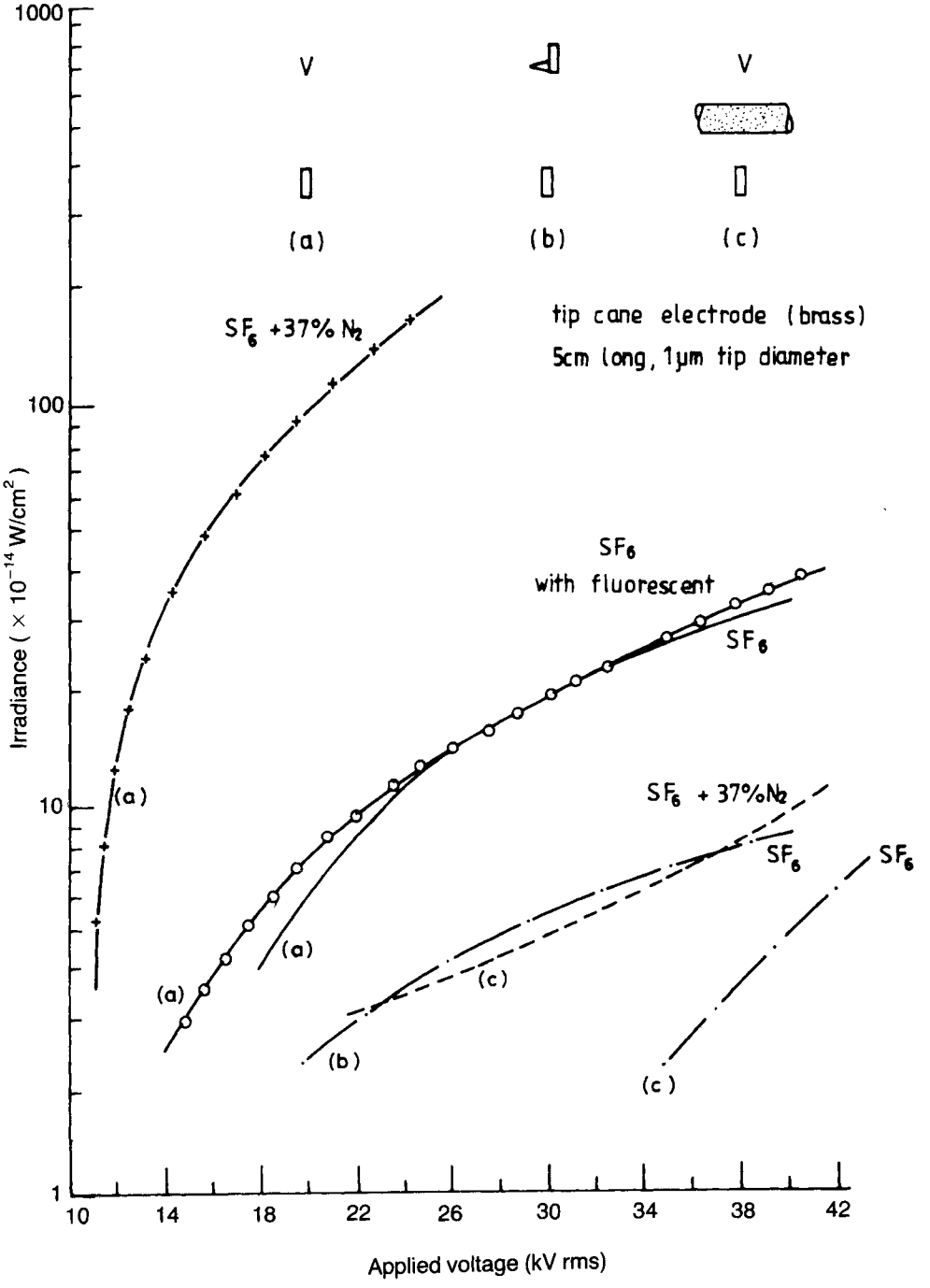

FIG. 9. Corona light detected in SF_6 and SF_6/N_2 mixtures for different experimental conditions at 0.3 bars.

SF_6 significantly improves the corona discharge light emission. The electron swarms in SF_6 on its own are not very luminous because of low excitation coefficient. Whereas N_2 has a very high excitation coefficient for second positive group radiation. The small admixtures of N_2 to SF_6 permit light emission from the corona discharge[19].

It should be pointed out that the actual discharge onset voltage for the tested electrode configurations is expected to be less than 14 kV since without the barrier, the discharge onset in SF_6 is detected at 14 kV (when the chamber walls are painted with fluorescent paint). To determine the inherent diaelectric strength of these mixtures, breakdown voltages (B.D.V.) were measured for a 2 mm gap for various mixtures. The measured values are given in Table 1 for mixtures containing 37% of the additive gas in each mixture. Thus, the results of Fig. 8 and Table 1 show that among the additives investigated, N_2 seems to have the best characteristics since its mixtures with SF_6 exhibit higher breakdown voltages as well as higher corona light emissions. Figure 9 shows the light emission behaviour for SF_6 and SF_6 + 37% N_2 mixtures for different electrode configurations. It is obvious that such mixtures exhibits higher irradiance magnitudes which make it possible to detect discharges which are even located in a hidden area. After investigating such mixtures having different percentage content of nitrogen, it was found that even mixtures containing as low as 2.5% of N_2 significantly improve the corona irradiance levels.

TABLE 1.

Gas	SF_6	SF_6 + Ar	SF_6 + He	SF_6 + Ne	SF_6 + N_2
B.D.V. (kV)	34.5	27.8	25	26	32.5

4. Conclusion

The light emission in SF_6 depends upon the applied voltage level, the gas pressure, the distance and angle of the corona point with respect to the fibre optic light guide cone angle, the radius of the active electrode, the material as well as the surface finish of the electrodes. The sensitivity of optical discharge detector can be enhanced by use of suitable fluorescent paint as well as gas additives. Mixtures of SF_6 with N_2 significantly improve the light emission and detection characteristics and with such mixtures, it is possible to detect the discharges which are even located in hidden areas. The results obtained in the present investigation are believed very useful for GIS industry as well as GIS development investigations.

References

[1] **Dale, S.** and **Wootton, R.**, Effect of fixed particle protrusions on 60 Hz and impulse breakdown voltage-pressure characteristics in SF_6, *3rd ISH, Milan, paper 32.10* (1979).

[2] **Cook, C., Wootton, R., Cookson, A.**, Influence of particles on AC and DC electrical performance of gas insulated systems at extra-high-voltage, *IEEE Trans.*, **PAS-96**(3): 768-777 (1977).

[3] **Carlson, G., Houston, J., Davis, W., Perry, M., Rautenberg, T.,** Fault sensors for SF_6 equipment, *Proc. 42nd American Power Conf.*, Chicago, **42**(111) April: 615-619 (1980).

[4] **Kusumoto, S., Itoh, S., Tsuchiya, Y., Mukae, H., Matsuda, S., Takahashi, K.,** Diagnostic technique of gas insulated substation of partial discharge detection, *IEEE Trans.*, **PAS-99**(4): 1456-1463 (1980).

[5] **Tominaga, S., Kunahara, H., Hirooka, K., Yoshioka, T.,** SF_6 gas analysis technique and its application for evaluation of internal conditions in SF_6 gas equipment, *IEEE Trans.*, **PAS-100**(9): 4196-4206 (1981).

[6] **Braun, J.** and **Chu, F.,** Novel low cost SF_6 arcing by-product detectors for field use in gas-insulated switchgear, *IEEE Trans.*, **PWRD-1**(2): 81-85 (1986).

[7] **Bartnikas, R.** and **McMahon, J.** (ed.), *Engineering Dielectrics,* Vol. 1, ASTM Press, USA, pp. 327-408 (1981).

[8] **Graybill, H., Cronin, J., Field, E.,** Testing of gas insulated substations and transmission systems, *IEEE Trans.*, **PAS-93**(1): 404-413 (1974).

[9] **Lundgaard, L., Hegerberg, R., Kulsetas, J., Rein, A.,** Ultrasonic detection of particle movement and partial discharges in gas insulated apparatus, *Proc. 3rd Int. Symp. on Gaseous Dielectrics, Knoxville, Tennessee, USA, March,* pp. 300-306 (1982).

[10] **Vanhaeren, R., Stone, G., Meehan, J., Kurtz, M.,** Preventing failure in outdoor distribution class metalclad switchgear, *IEEE Trans.*, **PAS-104**(10): 2706-2712 (1985).

[11] **Boggs, S., Ford, G., Madge, R.,** Coupling device for the detection of partial discharge in a gas insulated switchgear, *IEEE Trans.*, **PAS-100**(8): 3969-3973 (1981).

[12] **Boggs, S., Chu, F., Ford, G., Law, C.,** Improved diagnostic test and fault location techniques for gas insulated switchgear, *42nd American Power Conf.*, Chicago, April, **42**(110): 609-614 (1980).

[13] **Konig, D., Neumann, C., Suiter, H., Lipken, H.,** Partial discharge measurements of SF_6 insulated high voltage metal enclosed switchgear on site: A study based on fundamentals and experiences available up to now, *CIGRE,* **1**(23-09): 1-17 (1980).

[14] **Hill, J.** and **Cresswell, R.,** Partial discharge testing of HV metalclad compound filled switchgear in service in London, *IEE Conf. Publ.* **94:** 163-170 (1973).

[15] **Teich, T.** and **Bronston, D.,** Light emission from electron avalanches in electronegative gases and nitrogen, *IEE Conf. Publ. No. 90,* pp. 335-337 (1972).

[16] **Cox, B.,** Partial discharge detection in GIS by an optical technique, *Proc. Int. Symp. on GIS, Toronto, Canada, Sep., pp. 341-349* (1985).

[17] **Farish, O., Ibrahim, O., Kurimoto, A.,** Prebreakdown corona processes in SF_6 and SF_6/N_2 mixtures, *3rd ISH, Milan,* paper 31.15 (1979).

[18] **Ibrahim, O.** and **Farish, O.,** Negative-point breakdown and prebreakdown in SF_6 and SF_6/N_2 mixtures, *IEE Conf. Publ. No. 189, Part 1,* pp. 161-164 (1980).

[19] **Teich, T.** and **Braunlich, R.,** U.V. radiation from electron avalanches in SF_6 with small admixtures of nitrogen, *Gaseous Dielectrics,* IV, Pergamon Press, pp. 71-81 (1984).

[20] **Butler, A.,** Spectroscopic analysis of surface discharges over a dielectric material, *Final Year Project, Dept. of Elect., Eng., University of Salford,* England, May (1975).

العـــوامـل المـــؤثرة في الاكتشاف الإلكـــتروبصري للتفريغـــات الهاليـــة في غـــاز سادس فلوريد الكـــبريت

أنور حسن مفتي* ، دونالد فريد بنز و نذر هـ . مالك*****

*قسم الهندسة الكهربائية وهندسة الحاسبات ، كلية الهندسة ، جامعة الملك عبد العزيز
جـــــدة - المملكة العربية السعودية ؛

**قسم الهندسة الكهربائية ، كلية الهندسة ، جامعة سالفورد - المملكة المتحدة ؛

***قسم الهندسة الكهربائية ، كلية الهندسة ، جامعة الملك سعود
الريـــــاض - المملكة العربية السعودية

المستخلص . يقوم هذا البحث بشرح نظام الإلكتروبصري لاكتشاف التفريغات الهالية التي تحدث داخـل الأجهـزة المملوءة بغـاز سادس فلوريد الكـبريت . ولقـد تم إجـراء الفحوصات لاستخدام جهاز اكتشاف التفريغ من أجل دراسة تأثير القيم التجريبية المتعددة (وهي كميات متغيرة القيمة) على كمية الضوء الهالي المكتشف . كما تم توضيح أن الأشعة المقاسة الناتجة عن التفريغ الهالي تعتمد على مستوى الجهد المستعمل (المطبق) وضغط الغاز والمسـافـة الزاوية بين مصدر التفريغ الهالي والألياف البصرية الناقلة للضوء ونصف قطر ونوعية وسطح وخواص الأقطاب الكهربائية . إضافة إلى ذلك تم توضيح أن إضافة غاز سادس فلوريد الكبريت يحسن إلى حد كبير وهام انبثاق ضوء التفريغ الهالي ، ومن الممكن تحسين حساسية جهاز الاكتشاف أكثر عن طريق استخدام طلاء الفلورسنت على الجدران الداخلية لوعاء الضغط .